Original Article

JCBFM

Journal of Cerebral Blood Flow & Metabolism
2018, Vol. 38(3) 393–403

DOI: 10.1177/0271678X17699223
journals.sagepub.com/home/jcbfm
SAGE

^{11}C-DPA-713 has much greater specific binding to translocator protein 18 kDa (TSPO) in human brain than ^{11}C-(*R*)-PK11195

Masato Kobayashi[1], Teresa Jiang[1], Sanjay Telu[1], Sami S Zoghbi[1], Roger N Gunn[2,3], Eugenii A Rabiner[2], David R Owen[3], Qi Guo[2], Victor W Pike[1], Robert B Innis[1] and Masahiro Fujita[1]

Abstract

Positron emission tomography (PET) radioligands for translocator protein 18 kDa (TSPO) are widely used to measure neuroinflammation, but controversy exists whether second-generation radioligands are superior to the prototypical agent ^{11}C-(*R*)-PK11195 in human imaging. This study sought to quantitatively measure the "signal to background" ratio (assessed as binding potential (BP_{ND})) of ^{11}C-(*R*)-PK11195 compared to one of the most promising second-generation radioligands, ^{11}C-DPA-713. Healthy subjects had dynamic PET scans and arterial blood measurements of radioligand after injection of either ^{11}C-(*R*)-PK11195 (16 subjects) or ^{11}C-DPA-713 (22 subjects). To measure the amount of specific binding, a subset of these subjects was scanned after administration of the TSPO blocking drug XBD173 (30–90 mg PO). ^{11}C-DPA-713 showed a significant sensitivity to genotype in brain, whereas ^{11}C-(*R*)-PK11195 did not. Lassen occupancy plot analysis revealed that the specific binding of ^{11}C-DPA-713 was much greater than that of ^{11}C-(*R*)-PK11195. The BP_{ND} in high-affinity binders was about 10-fold higher for ^{11}C-DPA-713 (7.3) than for ^{11}C-(*R*)-PK11195 (0.75). Although the high specific binding of ^{11}C-DPA-713 suggests it is an ideal ligand to measure TSPO, we also found that its distribution volume increased over time, consistent with the accumulation of radiometabolites in brain.

Keywords

18 kDa (TSPO), positron emission tomography, rs6971 polymorphism, XBD173, metabolite-corrected arterial input

Received 20 September 2016; Revised 11 January 2017; Accepted 13 January 2017

Introduction

Translocator protein 18 kDa (TSPO) is highly expressed in inflammatory cells, including activated microglia, macrophages, and reactive astrocytes.[1] ^{11}C-PK11195 was the first PET radioligand developed to image TSPO,[2] and its higher affinity enantiomer, ^{11}C-(*R*)-PK11195,[3] has successfully imaged areas of inflammation in brain[4] and in the periphery.[5] Several second-generation ^{11}C-labeled radioligands have been developed to increase the specific (i.e. receptor-bound) component of brain uptake; these include ^{11}C-DAA1106,[6] ^{11}C-PBR28,[7] and ^{11}C-DPA-713.[8] These second-generation radioligands are widely thought to have greater "signal to background" ratio than ^{11}C-(*R*)-PK11195, based largely on full-blockade studies in monkeys. As a measure of signal to background, we used binding potential (BP_{ND}), which is the ratio at equilibrium of specific to non-displaceable uptake, and found that the BP_{ND} of ^{11}C-PBR28[9] in brain of rhesus macaques was 70-fold

[1]Molecular Imaging Branch, National Institute of Mental Health, National Institute of Health, Bethesda, MD, USA
[2]Imanova Ltd, London, UK
[3]Division of Brain Sciences, Department of Medicine, Imperial College, London, UK

The first two authors contributed equally to this work.

Corresponding author:
Masahiro Fujita, National Institute of Mental Health, Bldg. 10, Rm. B1D43, 10 Center Drive, MSC-1026, Bethesda, MD 20892-1026, USA.
Email: fujitam@mail.nih.gov

higher than that of ^{11}C-(*R*)-PK11195.[10] However, comparable blocking studies for ^{11}C-(*R*)-PK11195 have not been performed in human subjects. Instead, the BP_{ND} value for ^{11}C-(*R*)-PK11195 in human brain has been indirectly estimated with a pseudo-reference region[11] but never directly measured.

Imaging studies conducted with the second-generation radioligand ^{11}C-PBR28 found that the subject's genotype affected the affinity of radioligand binding to TSPO.[12] Specifically, the single nucleotide polymorphism (SNP) rs6971 generates a co-dominantly expressed genotype: homozygous high-affinity binder (HAB), homozygous low-affinity binder (LAB), and heterozygous mixed-affinity binder (MAB).[13] All second-generation radioligands tested to date are sensitive, more or less, to this polymorphism, with an in vitro affinity ratio of HAB to LAB of about 4:1 for DPA-713 and 50:1 for PBR28.[14] However, the sensitivity of ^{11}C-(*R*)-PK11195 to this genotype is unclear. Although in vitro receptor binding studies found that ^{11}C-(*R*)-PK11195 is insensitive to the genotype,[14] in vivo imaging results are inconsistent among organs. Whole-body imaging studies suggest that the brain is not sensitive to this genotype but that peripheral organs like lung and heart are.[10] However, these results were not based on full quantification using radiometabolite-corrected arterial input function; full quantification might be able to distinguish whether the brain is also sensitive to polymorphism rs6971.

This study sought to directly measure in humans the "signal to background ratio" (assessed as BP_{ND}) of ^{11}C-(*R*)-PK11195 using the receptor blocking drug XBD173[15,16] in humans, and to compare it with one of the most promising second-generation radioligands, ^{11}C-DPA-713. In previous studies, ^{11}C-DPA-713 was found to be superior to ^{11}C-(*R*)-PK11195 in a rodent model of neuroinflammation[17] and to ^{11}C-PBR28—a widely used second-generation radioligand—in patients with epilepsy.[18] We compared these two radioligands—^{11}C-(*R*)-PK11195 and ^{11}C-DPA-713—with regard to their sensitivity to polymorphism rs6971 and to their ability to absolutely quantify TSPO in brain as distribution volume (V_T).

Materials and methods

Radiopharmaceutical preparation

^{11}C-DPA-713 was synthesized as described previously[19] with high radiochemical purity (>99%) and a specific activity of 104 ± 57 GBq/μmol at the time of injection under our Investigational New Drug Application (IND) #116,950. ^{11}C-(*R*)-PK11195 was synthesized as previously described[10] with high radiochemical purity (>98%) and specific activity at time of injection of 104 ± 71 GBq/μmol under IND #101,908.

Subjects

This study was approved by the Institutional Review Board of the National Institutes of Health and adhered with the Helsinki Declaration of 1975 (and as revised in 1983); informed consent was obtained from all subjects. Twenty-two healthy volunteers (11 males, 11 females, 32 ± 9 years old) had ^{11}C-DPA-713 brain PET scans. The distribution of gender and affinity type was 9M/5F HABs, 1M/4F MABs, and 1M/2F LABs. Sixteen healthy volunteers (seven males, nine females, 32 ± 10 years old) had ^{11}C-(*R*)-PK11195 scans. The distribution of gender and affinity type was 1M/4F HABs, 4M/4F MABs, and 2M/1F LABs. All subjects were free of current medical or psychiatric illnesses based on medical history, physical examination, electrocardiogram, and laboratory blood and urine tests, which included a complete blood count, serum chemistries, thyroid function test, urinalysis, and urine drug screening. TSPO affinity type was determined by in vitro receptor binding to TSPO on leucocyte membranes or genetic analysis as previously described.[12]

Measuring ^{11}C-DPA-713 and ^{11}C-(R)-PK11195 in arterial blood

To determine arterial input function for brain PET scans, blood samples (1 mL each) were drawn from the radial artery at 15-s intervals until 2.5 min, followed by samples (3–11 mL) at 3, 4, 6, 8, 10, 15, 20, 30, 40, 50, 60, 75, and 90 min. The concentration of parent radioligand was measured using high-performance liquid chromatography (HPLC) after separating plasma from whole blood within a few minutes of blood sampling, as previously described.[20] The activity of whole blood was also measured.

Plasma concentration of the parent compound and whole blood activity were fitted to a triexponential function with weighting to minimize the relative distances of the measured values from the fitted values (relative weighting). For one subject who had ^{11}C-DPA-713 scans with and without XBD173, biexponential fitting was performed because triexponential fitting did not converge. The plasma-free fraction (f_P) was measured by ultrafiltration, as previously described.[21]

Scan procedures

Most PET scans were performed on an Advance Tomograph (GE Healthcare, UK) except three pairs of baseline scans and those after XBD173 administration using ^{11}C-DPA-713, where a high-resolution

research tomograph (HRRT) scanner (CTI, Knoxville, TN, USA) was used. All pairs of baseline and XBD173 blocked scans were performed on the same day. After injection of ^{11}C-DPA-713 or ^{11}C-(*R*)-PK11195 over 1 min, dynamic three-dimensional emission scans were acquired for 90 min. The dynamic data were separated into 27 frames of increasing duration from 30 s to 5 min. One transmission scan using ^{68}Ge or ^{137}Cs rod was acquired before radioligand injection. The position of the transmission scan was corrected for motion before applying attenuation correction. PET images were reconstructed with filtered back projection (Hanning filter with 4.0 cut-off) or ordered subset expectation maximization (two iterations and 30 subsets) for Advance Tomograph and HRRT, respectively. After image reconstruction, HRRT data were smoothed with 6.5 mm full-width-half-maximum using a Gaussian filter to match spatial resolution.

XBD173 administration

To induce partial blockade of radioligand binding to TSPO, XBD173 (401.5 g/mol) was administered orally ~105 min before injection of the PET ligand.[15] XBD173 was administered in six HABs who had ^{11}C-DPA-713 scans and all 16 subjects who had ^{11}C-(*R*)-PK11195 scans. Dosing occurred as follows: for ^{11}C-DPA-713 scans, 30 mg for three subjects, and 90 mg for three subjects; for ^{11}C-(*R*)-PK11195 scans, 45 mg for six subjects, and 90 mg for 10 subjects. We began with a dose of 45 mg for ^{11}C-(*R*)-PK11195; our goal was to achieve >50% receptor occupancy to accurately estimate non-displaceable uptake (V_{ND}). However, because ^{11}C-(*R*)-PK11195 scans showed variable receptor occupancy due to low levels of specific binding, we subsequently increased the dose to 90 mg for ^{11}C-(*R*)-PK11195. ^{11}C-DPA-713, which was studied later, showed greater BP_{ND}; thus, the lowest dose of 30 mg provided measurement of 71–100% receptor occupancy.

Brain image analysis

Image and kinetic analyses for brain PET images were performed using PMOD (version 3.6). All time frames of dynamic PET images were realigned for motion correction. After coregistering PET and a sagittal MR image of 1-mm contiguous slices obtained using a 3.0-T Achieva device (Philips Health Care, Andover, MA, USA), the images were spatially normalized to the MRI template in Montreal Neurological Institute (MNI) space. The PET data in the following volumes of interest (VOI) were obtained in the MNI space: frontal (432 cm^3), occipital (172 cm^3), parietal (247 cm^3), temporal (251 cm^3), medial temporal (36 cm^3), and cingulate (28 cm^3) cortices, thalamus (17 cm^3), caudate (16 cm^3), putamen (17 cm^3), cerebellum (195 cm^3), brainstem (6.5 cm^3), and white matter (8.3 cm^3).

Calculating distribution volume with radiometabolite-corrected arterial input function

V_T is an index of receptor density and equals the ratio at equilibrium of the concentration of radioligand in tissue to that in plasma. The concentration of radioligand in tissue represents the sum of specific binding (receptor-bound) and non-displaceable uptake (non-specifically bound and free radioligand in tissue water).[22]

Regional V_T values were calculated using an unconstrained two-tissue compartment model and Logan plot,[23] using the radiometabolite-corrected plasma input function. For the two-compartment model, brain data for each frame were weighted by assuming that the standard deviation/mean of the data was proportional to the inverse square root of noise equivalent counts; radioactivity in whole blood was used to correct brain data for the vascular component, assumed to be 5% of total brain volume. The delay between the arrival of ^{11}C-DPA-713 or ^{11}C-(*R*)-PK11195 in the radial artery and brain was estimated by fitting the whole brain. For Logan plot, weighting, delay, and consideration of the vascular component were not included as in the standard Logan plot analyses. The one-compartment model was not considered because previous studies had reported the superiority of the two-compartment model for both ^{11}C-DPA-713[8] and ^{11}C-(*R*)-PK11195.[24] Because almost all brain regions express TSPO, we did not apply a reference region method in the kinetic analysis.

Time–stability analysis

To determine the minimal scan length for reliable measurement and to indirectly assess whether ^{11}C-DPA-713 or ^{11}C-(*R*)-PK11195 radiometabolites enter the brain, the time–stability of V_T was examined by increasingly truncating the 90-min scan by 5-min increments to the shortest length of 0 to 40 min.

Estimating non-displaceable distribution volume

A modified Lassen plot was used to estimate the specific and non-displaceable components of ^{11}C-DPA-713 and ^{11}C-(*R*)-PK11195 in brain in two ways: (1) with Lassen occupancy plot using the difference in V_T at baseline and after partial blockade with XBD173 and (2) with the polymorphism plot (^{11}C-DPA-713 only) using the difference in V_T between two affinity types.[15,25] In general, the Lassen plot enables estimation of V_{ND} as *x*-intercept by measuring the linear relationship of

total uptake (V_T) as x-axis and specific binding (V_S) as y-axis in several brain regions. Here, V_S can be substituted with proportional variables:

(1) Lassen occupancy plot: V_T at baseline ($V_T^{Baseline}$) minus V_T after partial blockade (V_T^{Block}) for occupancy plot, under the assumption that V_{ND} and the percentage occupancy are the same across all regions

$$V_T^{Baseline} - V_T^{Block} = Occ \cdot (V_T^{Baseline} - V_{ND}) \quad (1)$$

Equation (1) indicates that the slope and x-intercept correspond to receptor occupancy and V_{ND}, respectively. To improve identifiability of V_{ND} for ^{11}C-DPA-713 and ^{11}C-(*R*)-PK11195, the regression was performed by constraining V_{ND} to be equal among HABs or MABs.

(2) Polymorphism plot: Group mean V_T for HABs (V_T^{HAB}) minus group mean V_T for MABs (V_T^{MAB}) for polymorphism plot, under the assumption that V_{ND} is uniform across all regions. Similar to the occupancy plot, this assumption leads to the following

$$V_T^{HAB} - V_T^{MAB} = \Delta \cdot (V_T^{HAB} - V_{ND}) \quad (2)$$

Equation (2) estimates both genetic effect (the slope) and a population average for V_{ND} (the x-intercept). The same plot was performed using data from the other pairs of affinity types, i.e. HABs vs. LABs and MABs vs. LABs.

Statistical analysis

The identifiability of V_T by the two compartment model was expressed as a percentage and equaled the ratio of the standard error (SE) of V_T divided by the value of V_T itself. A lower percentage indicates better identifiability. Repeated measures two-way analysis of variance was used to compare V_T among different affinity groups by using region as the repeating parameter within subjects. A value of $P < 0.05$ was considered significant. Linear regression for the modified Lassen occupancy and polymorphism plots was performed using Prism 5 (GraphPad Software, Inc., La Jolla, CA, USA). The other statistical analyses were performed with SPSS (version 22 for Windows; SPSS Inc., Chicago, IL, USA). Group data are expressed as mean ± SD.

Results

Pharmacologic effects

No adverse or clinically detectable pharmacologic effects were observed with either ^{11}C-DPA-713 (28 scans) or ^{11}C-(*R*)-PK11195 (32 scans), or in any of the 22 subjects (six and 16 subjects who had ^{11}C-DPA-713 and ^{11}C-(*R*)-PK11195 scans, respectively) who received XBD173. Supplemental Table 1 lists the administered doses of the PET ligands. No significant changes in heart rate, blood pressure, respiratory rate, or ECGs were observed during the PET scan nor in blood or urine test results repeated after the scan.

Kinetic analysis

The brain time–activity curves of ^{11}C-DPA-713 clearly showed its sensitivity to polymorphism rs6971, whereas ^{11}C-(*R*)-PK11195 showed no sensitivity (Figure 1). For HABs and MABs, ^{11}C-DPA-713 showed greater peak radioactivity uptake and slower washout than ^{11}C-(*R*)-PK11195, indicating the presence of greater specific binding of this second-generation radioligand.

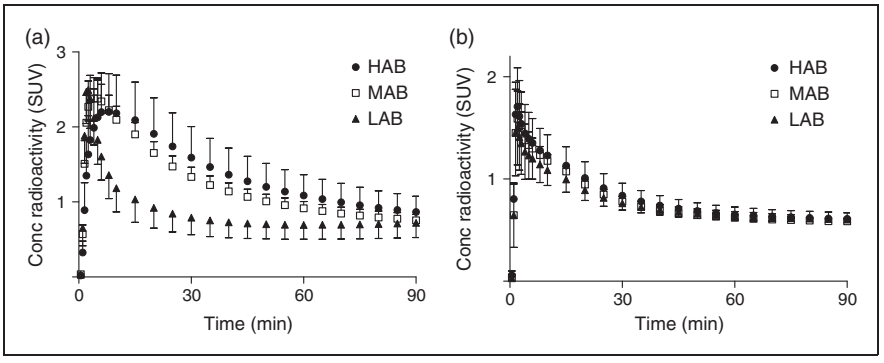

Figure 1. Mean brain radioactivity concentrations of ^{11}C-DPA713 (a) and ^{11}C-(*R*)-PK11195 (b) in each binder group. HABs: high-affinity binders; MABs: mixed-affinity binders; LABs: low-affinity binders. Error bars denote SD.

The kinetic analysis of brain and plasma data yielded three major findings. First, the Logan plot gave excellent fitting for all datasets (Supplemental Figure 1) and identified V_T well for both radioligands. In contrast, an unconstrained two-tissue compartment model failed to identify V_T well in some scans. For ^{11}C-DPA-713, the two-tissue compartment model poorly identified V_T (%SE $\geq$ 10) or failed to converge in three to nine of the 12 regions in five of 28 scans. For ^{11}C-(*R*)-PK11195, the two-tissue compartment model poorly identified V_T (%SE $\geq$ 10%) in three to seven regions in three of 32 scans. Because the Logan plot can underestimate V_T when the data are noisy, we compared it to the two-tissue compartment model in the datasets where the compartment model showed good identifiability of <10% SE. In fact, the Logan plot minimally underestimated V_T values: $-2.8 \pm 11.8\%$ for ^{11}C-DPA-713 and $-0.3 \pm 6.0\%$ for ^{11}C-(*R*)-PK11195. Thus, because the Logan plot identified V_T well in all regions and did not underestimate V_T, we used this non-compartmental approach to compare the two radioligands.

Table 1. Parameters of ^{11}C-DPA713 and ^{11}C-(*R*)-PK11195 in whole brain.

Parameters	^{11}C-DPA713	^{11}C-(*R*)-PK11195
V_T^{HAB} (mL cm^{-3})	3.61 ± 0.56	0.74 ± 0.14
V_T^{MAB} (mL cm^{-3})	1.94 ± 0.17	0.74 ± 0.16
V_T^{LAB} (mL cm^{-3})	1.21 ± 0.15	0.60 ± 0.18
V_{ND} (mL cm^{-3})	0.44 (0.34–0.53)	0.42 (0.31–0.53)

HABs: high-affinity binders; MABs: mixed-affinity binders; LABs: low-affinity binders; V_T: total distribution volume.
Note: Data are mean ± SD. Non-displaceable uptake (V_{ND}) was calculated from the occupancy plots of HABs.

The second major finding was that ^{11}C-DPA-713 showed significant sensitivity to genotype, whereas ^{11}C-(*R*)-PK11195 did not. Statistical analysis confirmed that V_T for HABs, MABs, and LABs differed significantly for ^{11}C-DPA-713 ($P = 0.001$, $F = 10.95$, $df = 2, 19$), but not for ^{11}C-(*R*)-PK11195 ($P = 0.37$, $F = 1.06$, $df = 2, 13$) (Table 1). For example, the whole brain V_T of ^{11}C-DPA-713 in HABs (3.6 ± 0.6 mL cm^{-3}) was about 1.9-fold higher than that in MABs (1.9 ± 0.2 mL cm^{-3}).

The third major finding was that V_T for both radioligands was unstable over time—i.e. V_T increased with increasing scan duration, consistent with the accumulation of radiometabolites in brain. The most sensitive condition for assessing the presence of radiometabolites is when there is little or low levels of specific receptor binding in brain by the parent radioligand to dilute the impact of radiometabolites. For this reason, we compared the time–stability of the radioligands in LABs and also in HABs after administration of XBD173 (Figure 2 and Table 2). During the last 40 min of the scan of LABs, V_T of whole brain increased by 25% for ^{11}C- DPA-713 and, similarly, by 26% for ^{11}C-(*R*)-PK11195. Scans of HABs after XBD173 administration showed a 13% increase for ^{11}C-DPA-713 and a larger 27% increase for ^{11}C-(*R*)-PK11195. Given that ^{11}C-DPA-713 has greater specific binding than ^{11}C-(*R*)-PK11195, this apparent effect of radiometabolites was diminished for ^{11}C-DPA-713 in HABs (Figure 2(a)). That is, during the same time interval, V_T of whole brain increased by only 8% for ^{11}C-DPA-713 but by 26% for ^{11}C-(*R*)-PK11195.

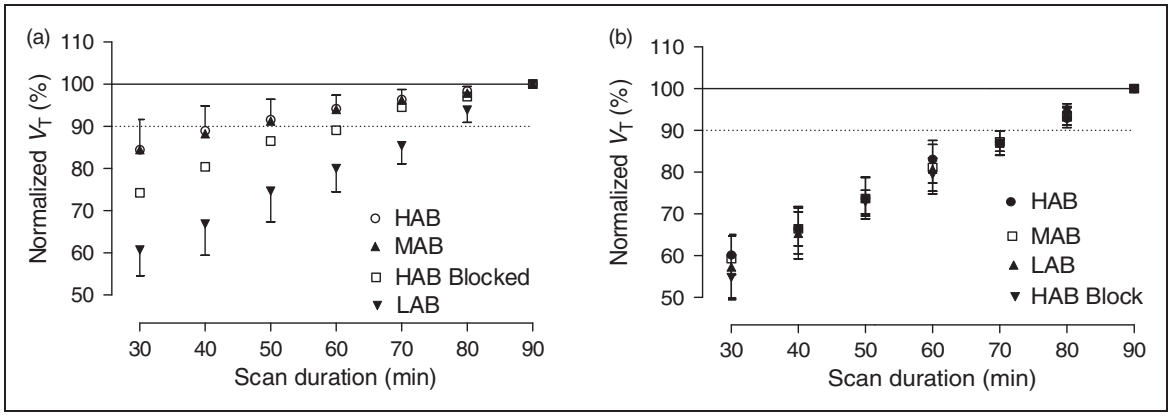

Figure 2. Time–stability analysis for kinetic analysis of ^{11}C-DPA713 (a) and ^{11}C-(*R*)-PK11195 (b). Total distribution volume (V_T) obtained from baseline scans for HABs, MABs, and LABs are plotted as a function of duration of image acquisition. V_T was calculated for whole brain using a Logan plot. V_T values are normalized as a percentage of terminal value attained from 90 min of imaging. The data represent mean ± SD of all three subjects.
HABs: high-affinity binders; MABs: mixed-affinity binders; LABs: low-affinity binders.

Estimating specific and non-displaceable uptake

For ^{11}C-DPA-713, BP_{ND} was estimated in two ways: by receptor blockade in HABs and by the so-called polymorphism plot, which compares the uptake between two affinity types.[15,25] After receiving XBD173, all six HABs showed marked blocking effects, both in plasma and in brain (Figure 3). In plasma, XBD173 significantly increased the concentration of ^{11}C-DPA-713, consistent with its blocking the distribution of the radioligand to peripheral organs.[10] In brain, receptor blockade increased peak radioactivity uptake (secondary to higher plasma concentrations), increased washout, and decreased total uptake over the 90-min scan. The Lassen occupancy plot of baseline and blocked scans showed an excellent linear regression and determined V_{ND} as 0.44 mL cm^{-3} with a 95% confidence interval of 0.34–0.53 and receptor occupancy (i.e. slope) of $91 \pm 12\%$ (Figure 4(a)). Based on the estimated V_{ND} (0.44), the ratio of specific to non-displaceable uptake (i.e. BP_{ND}) for whole brain was 7.3 ± 2.2, 3.4 ± 0.3, 1.8 ± 0.2 in HABs, MABs, and LABs, respectively.

Table 2. Comparison of four ^{11}C-radioligands to image translocator protein.

Ligand	V_T HABs (mL cm^{-3})	V_{ND}	BP_{ND} HABs (n)	BP_{ND} MABs (n)	BP_{ND} LABs (n)	Time stability[a] of V_T LABs (n)	Time stability[a] of V_T HABs after blockade (n)
^{11}C-DPA-713	3.6	0.44	7.3 (14)	3.4 (5)	1.8 (3)	25% (3)	13% (6)
^{11}C-(*R*)-PK11195	0.7	0.42	0.8 (5)	0.9 (8)	0.5 (3)	26% (3)	27% (5)

HABs: high-affinity binders; MABs: mixed-affinity binders; LABs: low-affinity binders; V_T: total distribution volume.
[a]% increase of V_T in last 40 min.

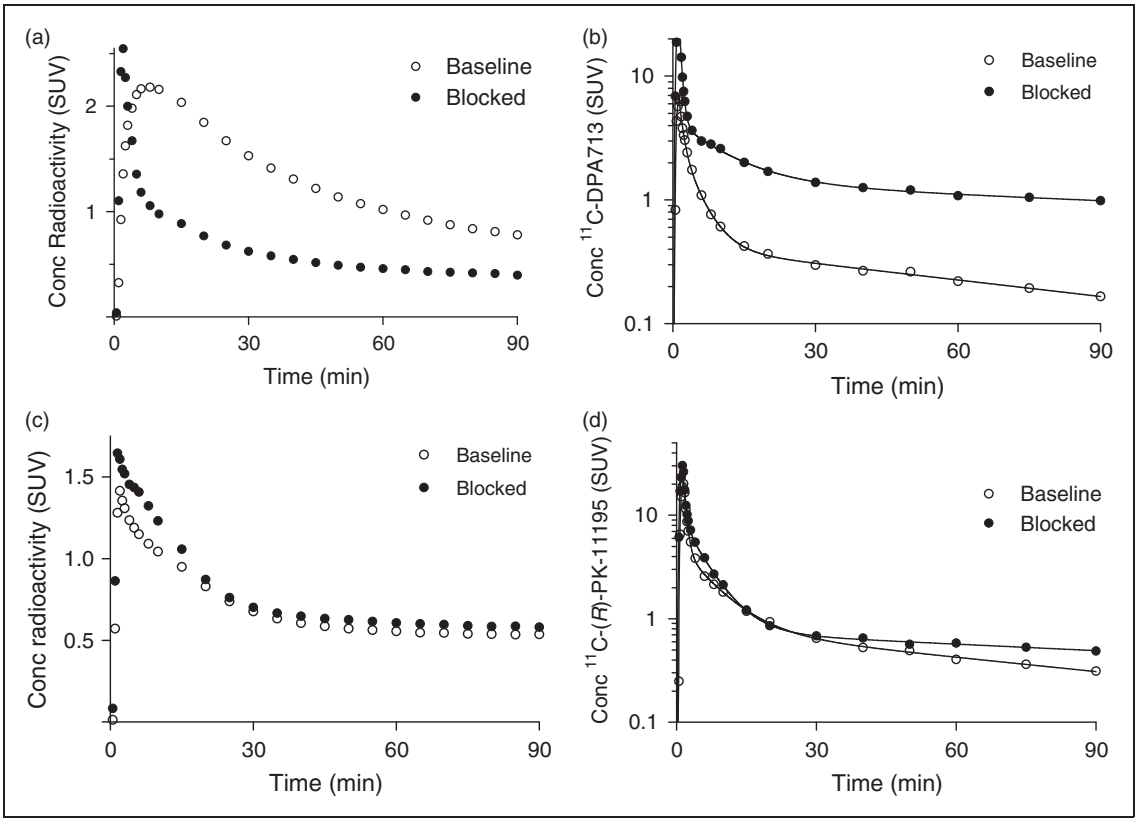

Figure 3. Data from a representative ^{11}C-DPA713 subject in whole brain (a) and arterial plasma (b) at baseline (○) and after blockade (●). Data from a representative ^{11}C-(*R*)-PK11195 subject in brain (c) and arterial plasma (d) at baseline (○) and after blockade (●). Blockade was done with 90 mg XBD173. Time courses of parent concentrations in arterial plasma were triexponentially fitted.

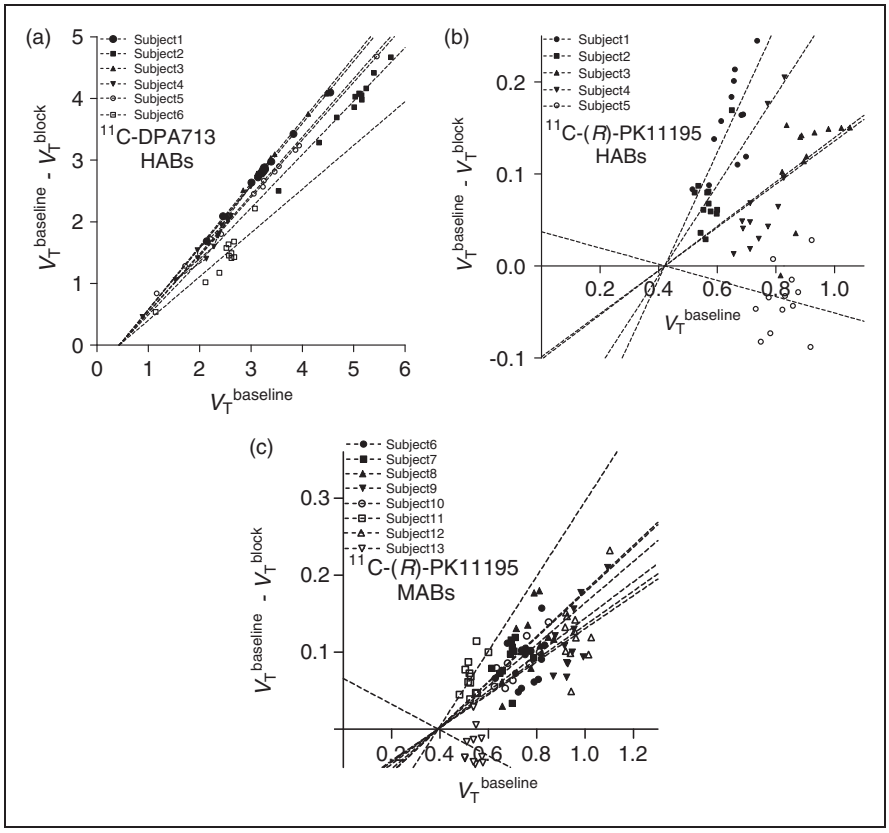

Figure 4. Lassen occupancy plot to determine non-displaceable uptake (V_{ND}) of ^{11}C-DPA713 in HABs (n = 6; a) and that of ^{11}C-(*R*)-PK11195 in HABs (n = 5; b) and MABs (n = 8; c). Each point represents a brain region in an individual subject. HABs: high-affinity binders; MABs: mixed-affinity binders.

The polymorphism plot, which was the second method of estimating the BP_{ND} of ^{11}C-DPA-713, showed excellent fit for all three combinations of the genotypes (Figure 5). V_{ND} and its 95% confidence interval (in parentheses) was 1.21 (0.87–1.56) for HABs–MABs, 0.88 (0.32–1.44) for HABs–LABs, and 0.99 (0.76–1.23) for MABs–LABs. The average (1.03) of these three V_{ND} values from the polymorphism plot was 2.3 times that obtained via the Lassen occupancy plot (0.44). BP_{ND} of whole brain was 2.59 ± 1.32 for HABs, 0.88 ± 0.36 for MABs, and 0.18 ± 0.41 for LABs. Largely because of the higher values of V_{ND} from the polymorphism plot, the BP_{ND} values from the genetic analysis were about one-third those obtained via the Lassen occupancy plot (Table 1). The cause for the different V_{ND} by Lassen occupancy and polymorphism plots is unclear but possibilities are the small sample size and intersubject variability in V_{ND}, including possible differences among different affinity types.

For ^{11}C-(*R*)-PK11195, BP_{ND} was estimated with only receptor blockade because ^{11}C-(*R*)-PK11195 showed no significant sensitivity to genotype (Table 1). ^{11}C-(*R*)-PK11195 showed relatively small blocking effects from XBD173, both in plasma and brain (Figure 3), consistent with ^{11}C-DPA-713 having greater specific binding in brain and periphery. The Lassen occupancy plot of baseline and blocked scans determined V_{ND} well as 0.42 (95% C.I.: 0.31–0.53) and 0.39 mL cm^{-3} (95% C.I.: 0.28–0.51) for HABs and MABs, respectively (Figure 4(b) and (c)). However, this good identifiability of V_{ND} was achieved only by constraining V_{ND} to be equal among HABs (Figure 4(b)) or MABs (Figure 4(c)) because of noisy data due to low specific binding in baseline scans. Receptor occupancy was $31\% \pm 29\%$ in HABs and $23\% \pm 18\%$ in MABs. Using V_{ND} values from these Lassen occupancy plots (0.42 for HABs and 0.39 for MABs), we calculated that the ratio of specific to non-displaceable BP_{ND} for whole brain was 0.75 ± 0.32 in five HABs and 0.89 ± 0.40 in MABs. Because XBD173 binding is affected by the rs6971 SNP,[26] the three LABs who received XBD173 showed no measurable binding blockade. When using the average V_{ND} in HABs and MABs, BP_{ND} in whole brain in LABs was 0.48 ± 0.44.

Because only free ligand enters the brain, V_T/f_P theoretically reflects receptor binding more accurately than V_T, although the additional measurement of f_P may

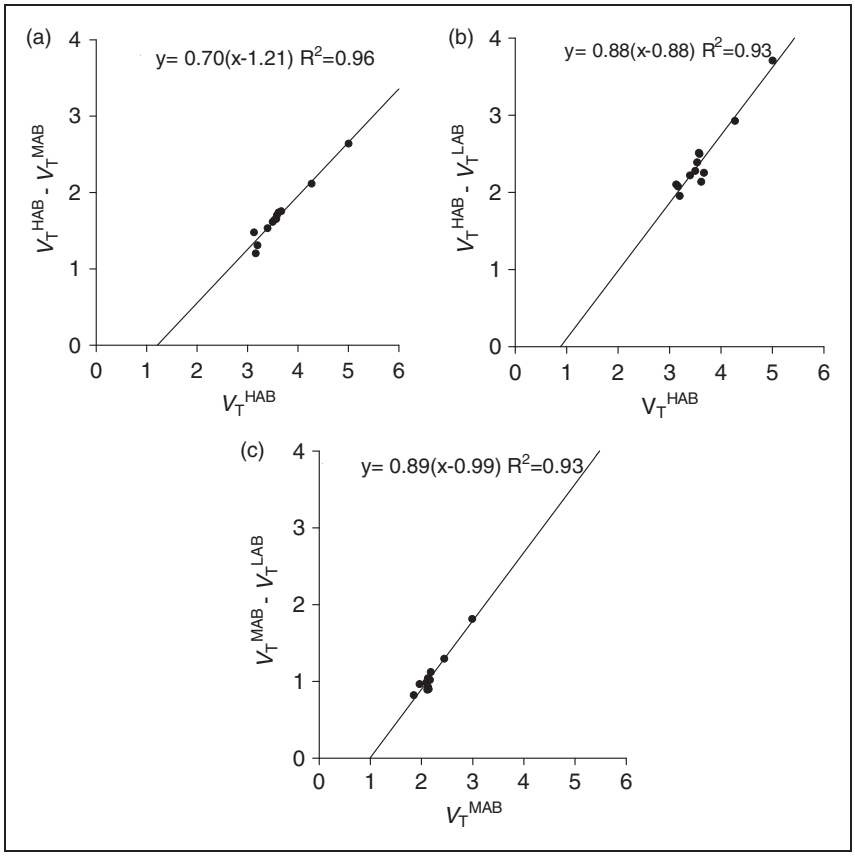

Figure 5. Polymorphism plot to determine a population average of non-displaceable uptake (V_{ND}) of ^{11}C-DPA713 in 14 HABs, five MABs, and three LABs. The plots were performed for three different combinations of the affinity types, HABs and MABs (a), HABs and LABs (b), and MABs and LABs (c). The plots were performed using average V_T values in each volume of interest (VOI) of the same affinity type.

decrease precision. XBD173 might have slightly altered f_P for both ^{11}C-DPA-713 and ^{11}C-(*R*)-PK11195 (Supplemental Table 2). Therefore, Lassen occupancy plots were performed using V_T/f_P. For ^{11}C-DPA-713, both occupancy (Supplemental Figure 2(a)) and polymorphism (Supplemental Figure 3) plots showed a linear regression with high R^2 and narrow confidence intervals for *x*-intercept, which were similar to the plots obtained using V_T. For occupancy plot, BP_{ND} was similar regardless of whether V_T/f_P or V_T was used: 7.4 for HABs using V_T/f_P (Supplemental Table 3) vs. 7.3 using V_T (Table 2). The polymorphism plot using V_T/f_P yielded a BP_{ND} of 3.9 for HABs vs. 2.6 using V_T. For ^{11}C-(*R*)-PK11195, the occupancy plot obtained using V_T/f_P provided a good linear regression with high R^2 and a narrow confidence interval for HABs (Supplemental Figure 2(b)) but not for MABs (Supplemental Figure 2(c)). One MAB showed a paradoxical 55% increase in V_T/f_P after binding blockade, but this may have been due to f_P measurement errors; occupancy plot was therefore performed after eliminating this subject (Supplemental Figure 2(d)). The occupancy plots for HABs (Supplemental Figure 2(b)) and MABs (Supplemental Figure 2(d)) yielded V_{ND}/f_P of 54 and 44 for HABs and MABs, respectively. BP_{ND} for HABs was 1.3 (Supplemental Table 3), which was greater than the 0.75 obtained using V_T (Table 1).

Discussion

^{11}C-DPA-713 was markedly superior to ^{11}C-(*R*)-PK11195 for quantifying TSPO in healthy human brain. With regard to perhaps the single most important comparison, the BP_{ND} (signal to background ratio) of HABs for ^{11}C-DPA-713 was about 10 times greater than that for ^{11}C-(*R*)-PK11195. Comparing the accumulation of radiometabolites in brain was more complicated. In LABs (who are most sensitive to radiometabolites in brain), both radioligands had similar time instability of V_T during the last 40 min of the scan. However, in HABs and MABs (which comprise

roughly 95% of our subjects screened to date), ^{11}C-DPA-713 showed better time stability of V_T than ^{11}C-(*R*)-PK11195. This differential effect of genotype was expected, as ^{11}C-DPA-713 has much greater specific binding of parent radioligand, which dilutes the effects of radiometabolites. Furthermore, because of its much greater BP_{ND}, ^{11}C-DPA-713 should be more sensitive than ^{11}C-(*R*)-PK11195 for detecting small changes in TSPO.

Sensitivity to genotype

^{11}C-DPA-713 showed a clear sensitivity to genotype. Specifically, V_T (mL cm^{-3}) was highest in HABs (3.61), then MABs (1.94), then LABs (1.21), and V_{ND} was estimated by occupancy plot to be 0.44. In contrast, no statistically significant differences between the three genotypes were observed with ^{11}C-(*R*)-PK11195, indicating that in vivo ^{11}C-(*R*)-PK11195 binding in brain is insensitive to genotype. However, the observed insensitivity must be interpreted with caution for several reasons. First, the sample sizes in this study may have been too small to detect a minor sensitivity. Second, because the "signal to background" ratio of ^{11}C-(*R*)-PK11195 was quite small ($BP_{ND} = 0.75$), and because brain uptake was low (peaking at only 1.5 SUV), the PET data may have lacked the sensitivity to detect an existing genotype effect. In fact, the noise associated with ^{11}C-(*R*)-PK11195 was evident in other measurements. For example, the scatter associated with the occupancy plot was greater for ^{11}C-(*R*)-PK11195 than for ^{11}C-DPA-713 (Figure 4).

While the present study found no sensitivity to genotype of ^{11}C-(*R*)-PK11195 in brain, we previously reported substantial sensitivity of this radioligand in several peripheral organs, including lung, spleen, and kidney.[10] Although genetic sensitivity may vary among organs, a more conservative interpretation is that the radioligand's high non-specific uptake (i.e. low specific binding) in brain obscured a sensitivity that actually exists and would be detected in a much larger sample size. That is, only organs with a very strong specific signal, like lung, spleen, and kidney, are able to detect the genetic effect in small sample sizes.

Instability of receptor measurements over time

Under tracer concentrations of radioligand, V_T is described by the following formula.

$$V_T = (B_{max}/K_D) \bullet f_P + V_{ND}$$

Because receptor density (B_{max}) and the affinity ($1/K_D$) of the radioligand for the receptor occur independently of time (i.e. are not expected to change during the course of a 90-min scan), V_T should also not depend on time if V_{ND} is independent of time. However, because of noise in the PET and plasma data, a minimal number of time points are required to identify V_T, which should then be stable using the remainder of the data. However, we found that V_T of both ^{11}C-(*R*)-PK11195 and ^{11}C-DPA-713 increased with increased scan duration, showing that the input of parent radioligand itself could not explain brain uptake. For example, V_T in LABs for both radioligands increased by about 25% during the last 40 minutes of the scan (Figure 2). One common cause of time instability is the accumulation of radiometabolites in brain, which would not be explained by an input function of only the parent radioligand. Thus, comparisons of V_T between individuals or groups might be secondary to differences in the metabolism of the radioligand and not the density of receptors in brain. Thus, caution should be used when either of these radioligands is used to measure TSPO in LABs. The very high specific binding of ^{11}C-DPA-713 obviates this concern for HABs and MABs, as potential radiometabolites are such a small percentage of total brain uptake. For example, the V_T of ^{11}C-DPA-713 in HABs increased by only 8% during the last 40 min of the scan.

Conclusion

^{11}C-DPA-713 was markedly superior to ^{11}C-(*R*)-PK11195 for quantifying TSPO in healthy human brain. The BP_{ND} value ("signal to background") of ^{11}C-DPA-713 was 10 times that of ^{11}C-(*R*)-PK11195 in HABs. The very low specific binding of ^{11}C-(*R*)-PK11195 in brain ($BP_{ND} = 0.75$) may explain why its sensitivity to genotype has only been detected in peripheral organs, like lung, that have much higher density of TSPO than that in brain.[10] Although the high specific binding of ^{11}C-DPA-713 suggests it is an ideal ligand to measure TSPO, we also found that its V_T increased over time, consistent with the accumulation of radiometabolites in brain. Although this putative accumulation of radiometabolites is a small percentage of brain uptake in HABs and MABs, it is a significant problem for LABs, who may need to be excluded from clinical studies.

Funding

The author(s) disclosed receipt of the following financial support for the research, authorship, and/or publication of this article: This study was funded by the Intramural Research Program of the National Institute of Mental Health, NIH (project numbers ZIAMH002852 and ZIAMH002793 under clinical protocols NCT02147392 and NCT02147392) and as a public–private partnership supported by the NIMH and the Foundation for the NIH Biomarkers Consortium (www.biomarkersconsortium.org).

Acknowledgements

We thank Mohammad B Haskali, Talakad G Lohith, Stal Shrestha, Maria D Ferraris Araneta, Denise Rallis-Frutos, Emily Page, Jeih-San Liow, Kimberly J. Jenko, Aneta Kowalski, Emily Fennell, Sanche Mabins, and the staff of the PET Department for successfully completing the studies, Ioline Henter for providing excellent editorial assistance, and Katharine Henry for assisting with data analysis.

Declaration of conflicting interests

The author(s) declared the following potential conflicts of interest with respect to the research, authorship, and/or publication of this article: R.N.Gunn and E.A. Rabiner are employees of Imanova Ltd.

Authors' contributions

Masato Kobayashi, Teresa Jiang, Sanjay Telu, and Sami S Zoghbi substantially contributed to acquisition, analysis, and interpretation of data; drafted the article and revised it critically for important intellectual content; and gave final approval for this version of the manuscript.

Roger N Gunn, Eugenii A Rabiner, David R Owen, Qi Guo, Victor W Pike, and Robert B Innis substantially contributed to the conception and design of the study; drafted the article and revised it critically for important intellectual content; and gave final approval for this version of the manuscript.

Masahiro Fujita substantially contributed to the conception and design of the study; contributed substantially to the acquisition, analysis, and interpretation of data; drafted the article and revised it critically for important intellectual content; and gave final approval for this version of the manuscript.

Supplementary material

Supplementary material for this paper can be found at the journal website: http://journals.sagepub.com/home/jcb

References

1. Papadopoulos V, Baraldi M, Guilarte TR, et al. Translocator protein (18 kDa): new nomenclature for the peripheral-type benzodiazepine receptor based on its structure and molecular function. *Trends Pharmacol Sci* 2006; 27: 402–409.
2. Camsonne R, Crouzel C, Comar D, et al. Synthesis of N-[^{11}C]methyl, N-(methyl-1-propyl), (chloro-2-phenyl)-1-isoquinoline carboxamide-3 (PK11195): a new ligand for peripheral benzodiazepine receptors. *J Labelled Compd Radiopharm* 1984; 21: 985–991.
3. Shah F, Hume SP, Pike VW, et al. Synthesis of the enantiomers of [N-methyl-^{11}C]PK 11195 and comparison of their behaviours as radioligands for PK binding sites in rats. *Nucl Med Biol* 1994; 21: 573–581.
4. Cagnin A, Kassiou M, Meikle SR, et al. Positron emission tomography imaging of neuroinflammation. *Neurotherapeutics* 2007; 4: 443–452.
5. van der Laken CJ, Elzinga EH, Kropholler MA, et al. Noninvasive imaging of macrophages in rheumatoid synovitis using ^{11}C-(*R*)-PK11195 and positron emission tomography. *Arthritis Rheum* 2008; 58: 3350–3355.
6. Zhang MR, Kida T, Noguchi J, et al. [^{11}C]DAA1106: radiosynthesis and in vivo binding to peripheral benzodiazepine receptors in mouse brain. *Nucl Med Biol* 2003; 30: 513–519.
7. Briard E, Zoghbi SS, Imaizumi M, et al. Synthesis and evaluation in monkey of two sensitive ^{11}C-labeled aryloxyanilide ligands for imaging brain peripheral benzodiazepine receptors in vivo. *J Med Chem* 2008; 51: 17–30.
8. Endres CJ, Pomper MG, James M, et al. Initial evaluation of ^{11}C-DPA-713, a novel TSPO PET ligand, in humans. *J Nucl Med* 2009; 50: 1276–1282.
9. Imaizumi M, Briard E, Zoghbi SS, et al. Brain and whole-body imaging in nonhuman primates of [^{11}C]PBR28, a promising PET radioligand for peripheral benzodiazepine receptors. *Neuroimage* 2008; 39: 1289–1298.
10. Kreisl WC, Fujita M, Fujimura Y, et al. Comparison of [^{11}C]-(*R*)-PK 11195 and [^{11}C]PBR28, two radioligands for translocator protein (18 kDa) in human and monkey: implications for positron emission tomographic imaging of this inflammation biomarker. *NeuroImage* 2010; 49: 2924–2932.
11. Kropholler MA, Boellaard R, Schuitemaker A, et al. Evaluation of reference tissue models for the analysis of [^{11}C](*R*)-PK11195 studies. *J Cereb Blood Flow Metab* 2006; 26: 1431–1441.
12. Kreisl WC, Jenko KJ, Hines CS, et al. A genetic polymorphism for translocator protein 18 kDa affects both in vitro and in vivo radioligand binding in human brain to this putative biomarker of neuroinflammation. *J Cereb Blood Flow Metab* 2013; 33: 53–58.
13. Owen DR, Howell OW, Tang SP, et al. Two binding sites for [^{3}H]PBR28 in human brain: implications for TSPO PET imaging of neuroinflammation. *J Cereb Blood Flow Metab* 2010; 30: 1608–1618.
14. Owen DR, Gunn RN, Rabiner EA, et al. Mixed-affinity binding in humans with 18-kDa translocator protein ligands. *J Nucl Med* 2011; 52: 24–32.
15. Owen DR, Guo Q, Kalk NJ, et al. Determination of [^{11}C]PBR28 binding potential in vivo: a first human TSPO blocking study. *J Cereb Blood Flow Metab* 2014; 34: 989–994.
16. Rupprecht R, Rammes G, Eser D, et al. Translocator protein (18 kD) as target for anxiolytics without benzodiazepine-like side effects. *Science* 2009; 325: 490–493.
17. Doorduin J, Klein HC, Dierckx RA, et al. [^{11}C]-DPA-713 and [^{18}F]-DPA-714 as new PET tracers for TSPO: a comparison with [11C]-(R)-PK11195 in a rat model of herpes encephalitis. *Mol Imaging Biol* 2009; 11: 386–398.
18. Gershen LD, Zanotti-Fregonara P, Dustin IH, et al. Neuroinflammation in temporal lobe epilepsy measured using positron emission tomographic imaging of translocator protein. *JAMA Neurol* 2015; 72: 882–888.
19. James ML, Fulton RR, Henderson DJ, et al. Synthesis and in vivo evaluation of a novel peripheral benzodiazepine receptor PET radioligand. *Bioorg Med Chem* 2005; 13: 6188–6194.

20. Zoghbi SS, Shetty HU, Ichise M, et al. PET imaging of the dopamine transporter with ^{18}F-FECNT: a polar radiometabolite confounds brain radioligand measurements. *J Nucl Med* 2006; 47: 520–527.
21. Gandelman MS, Baldwin RM, Zoghbi SS, et al. Evaluation of ultrfiltration for the free fraction determination of single photon emission computed tomography (SPECT) tracers: ß-CIT, IBF, and iomazenil. *J Pharm Sci* 1994; 83: 1014–1019.
22. Innis RB, Cunningham VJ, Delforge J, et al. Consensus nomenclature for in vivo imaging of reversibly binding radioligands. *J Cereb Blood Flow Metab* 2007; 27: 1533–1539.
23. Logan J, Fowler JS, Volkow ND, et al. Graphical analysis of reversible radioligand binding from time-activity measurements applied to [N-^{11}C-methyl]-(-)cocaine PET studies in human subjects. *J Cereb Blood Flow Metab* 1990; 10: 740–747.
24. Kropholler MA, Boellaard R, Schuitemaker A, et al. Development of a tracer kinetic plasma input model for (*R*)-[^{11}C]PK11195 brain studies. *J Cereb Blood Flow Metab* 2005; 25: 842–851.
25. Cunningham VJ, Rabiner EA, Slifstein M, et al. Measuring drug occupancy in the absence of a reference region: the Lassen plot re-visited. *J Cereb Blood Flow Metab* 2010; 30: 46–50.
26. Owen DR, Lewis AJ, Reynolds R, et al. Variation in binding affinity of the novel anxiolytic XBD173 for the 18 kDa translocator protein in human brain. *Synapse* 2011; 65: 257–259.